

# Cellular automaton model to simulate nucleation and growth of ferrite grains for low-carbon steels

L. Zhang

College of Science, Northeastern University, Shenyang 110006, People's Republic of China, and Shenyang National Laboratory for Materials Science, Institute of Metal Research, Chinese Academy of Sciences, Shenyang 110016, People's Republic of China

C.B. Zhang

The State Key Laboratory of Rolling and Automation, Northeastern University, Shenyang 110006, People's Republic of China, and College of Science, Northeastern University, Shenyang 110006, People's Republic of China

Y.M. Wang

Shenyang National Laboratory for Materials Science, Institute of Metal Research, Chinese Academy of Sciences, Shenyang 110016, People's Republic of China

X.H. Liu and G.D. Wang

The State Key Laboratory of Rolling and Automation, Northeastern University, Shenyang 110006, People's Republic of China

(Received 29 January 2002, accepted 3 June 2002)

A two-dimensional cellular automaton model was developed for the simulation of nucleation and growth of ferrite grains at various cooling rates in low-carbon steels. The model calculates the diffusion of the solute and temperature fields in an explicit finite method and incorporates local temperature and concentration changes into a nucleation or growth function, which is utilized by the automaton in a probabilistic fashion. The modeling provides an efficient way to understand how those physical processes dynamically progress and affect nucleation and growth of ferrite grains.

## I. INTRODUCTION

Because microstructures of low-carbon steels, especially their grain sizes of ferrite, have strong influence on their mechanical properties, considerable industrial importance is placed on predicting a  $\gamma$ - $\alpha$  phase transformation of steels during heat treatment. In controlled rolling, which is an optimized reheating, hot rolling, and cooling process, the chief aim is to obtain the microstructures consisting of small and uniform ferrite grains, which have favorable mechanical properties in general, and in particular yield preferable strength and toughness. In recent years, many efforts have been undertaken to understand how to obtain the refinement microstructure of ferrite grains.<sup>1-6</sup> However, the microstructure formation in steels is not yet fully understood because of the complexity of the solid-state transformation involving the combined complex behavior of heat-mass transfer, nucleation and growth etc., in the liquid and/or solid states and their interfaces during the  $\gamma$ - $\alpha$  phase transformation. Although experimental observations could qualitatively explain the microstructure formation without using modeling, quantitative understanding of this combined behavior and its dynamic dependence on temperature and composition of steels is required to control the

microstructure formation and in turn, the mechanical and physical properties of products by modeling. In these modeling works, Umemoto *et al.* studied the effect of cooling rate and austenite grain size on the resultant ferrite grain size.<sup>1,2</sup> Jacot and Rappaz provided a two-phase model for the prediction of microstructural evolution in an Fe-C alloy, which undergoes a diffusive phase transformation.<sup>3</sup> However, their works could not provide an complete understanding of nucleation and growth of ferrite grains.

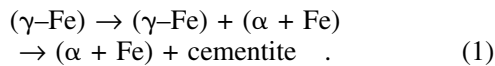
In fact, nucleation and growth of grains has been simulated in solidification by using a method called cellular automation (CA).<sup>7-10</sup> According to Wolfram,<sup>11</sup> CA could be an alternative model for solving the problems for systems with small degrees of freedom, typically handled by differential equations, or complex systems with large degrees of freedom. There are five distinct characteristics of CA: (i) There exists a grid of uniform cells, (ii) which are updated every time step (iii) with a finite value or state (iv) using deterministic rules, and (v) every cell is connected to a neighborhood of surrounding cells that control its evolution in time.

Thus, if nucleation and growth of grains could be simulated by the CA technique in solidification, why could it not be used to predict the phase transformation,

from austenite to ferrite, involved with nucleation and growth of ferrite grains in low-carbon steels? The aim of the present work is to establish a two-dimensional CA model that predicts nucleation and growth of ferrite grains for low carbon steels Fe- $\Sigma X_i$ -C (here  $X_i = \text{Si, Mn, Ni, Cu, Cr}$ ). The model uses an explicit finite volume technique to calculate the solutal and thermal fields. The local temperature and concentration changes are incorporated into a nucleation or growth function, which is used by the automaton in a probabilistic fashion within a small representative specimen. In addition, the simulated results are verified by the experimental results.<sup>2</sup>

## II. MATHEMATICAL DESCRIPTION

With respect to an Fe- $\Sigma X_i$ -C multicomponent alloy with a given low carbon concentration  $c$ , Fe- $\Sigma X_i$  could be regarded as a super-element  $S$ ;<sup>12</sup> thus the multicomponent  $S$ -C alloy is similar to a low-carbon Fe-C alloy. As a temperature in a local zone of the  $S$ -C alloy specimen is decreased at a given cooling rate, the phase transformations would take place:



For the Fe-C alloy with the concentration  $c$ , it is assumed that the equilibrium temperature beginning at a  $\gamma \rightarrow \alpha$  phase transformation  $A_{e3}$  is a temperature on the  $\gamma$ -phase line of an Fe-C phase diagram corresponding to the concentration  $c$  as shown in Fig. 1.

### A. The $\gamma \rightarrow \alpha$ phase transformation under continuous cooling

The  $\gamma \rightarrow \alpha$  phase transformation under continuous cooling could be considered as the sum of short-time isothermal holdings at successive temperatures as shown

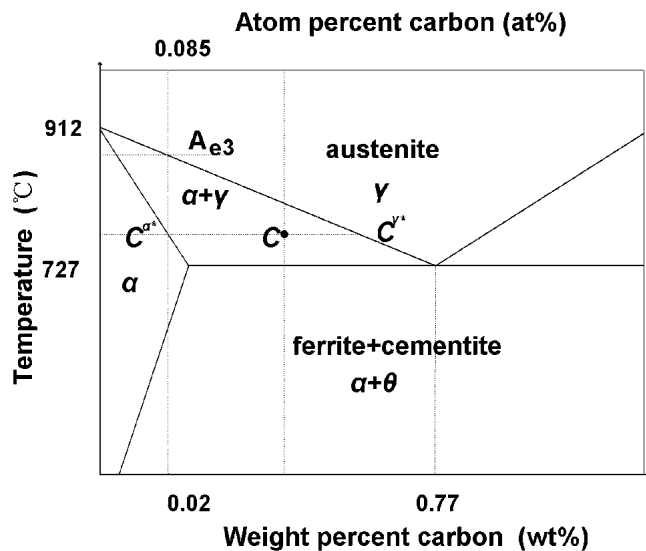


FIG. 1. Phase diagram of a Fe-C alloy.

in Fig. 2. It could be assumed, as observed in experiments, that ferrite grains nucleate preferentially on grain boundaries of austenite. In such cases, ferrite grains will initially nucleate on the grain boundaries of austenite, then the nucleated ferrite grains grow into the inner part of the austenite grains (as shown in Fig. 3). During continuous cooling from  $T_e$  to  $T$ , the number of newly formed ferrite grains  $n^1$  is

$$n(T) = \int_T^{T_e} \frac{I(T')[1-f]}{Q} dT' \quad (2)$$

Here  $I(T')$  is ferrite nucleation rate per unit area of austenite grain boundary at a temperature  $T'$ ,  $f$  is a grain boundary area fraction occupied by the ferrite grains, and  $Q$  is a cooling rate.

At the temperature  $T'$ , the ferrite nucleation rate  $I$  is expressed as

$$I = K_1(kT')^{-1/2} D_\gamma \exp\left(-\frac{K_2}{RT'(\Delta G_N^{\gamma \rightarrow \alpha + \gamma 1})^2}\right), \quad (3)$$

where  $D_\gamma$  is the carbon diffusivity in austenite,  $K_1$  is a constant related to the nucleation site density,  $K_2$  is a constant related to the austenite/ferrite interfacial energy,  $k$  is Boltzmann's constant, and  $\Delta G_N^{\gamma \rightarrow \alpha + \gamma 1}$  is a driving force of ferrite nucleation. It will be described in Sec. II.B.

### B. Driving force of ferrite nucleation

The driving force of ferrite nucleation  $\Delta G_{N(\text{Fe})}^{\gamma \rightarrow \alpha + \gamma 1}$  of the Fe-C alloy is calculated by  $\Delta G_{N(\text{Fe})}^{\gamma \rightarrow \alpha + \gamma 1} = \Delta G_{\text{Fe}}^{\gamma \rightarrow \alpha} - RT \ln a_{\text{Fe}}^\gamma$ , where  $\Delta G_{\text{Fe}}^{\gamma \rightarrow \alpha}$  is a free energy change of Fe in the  $\gamma \rightarrow \alpha$  phase transformation, and  $a_{\text{Fe}}^\gamma$  is an activity coefficient of Fe in austenite. For the Fe- $\Sigma X_i$ -C alloy presented in the simulation, because Fe- $\Sigma X_i$  has been regarded as the super-element  $S$ , which is similar to a

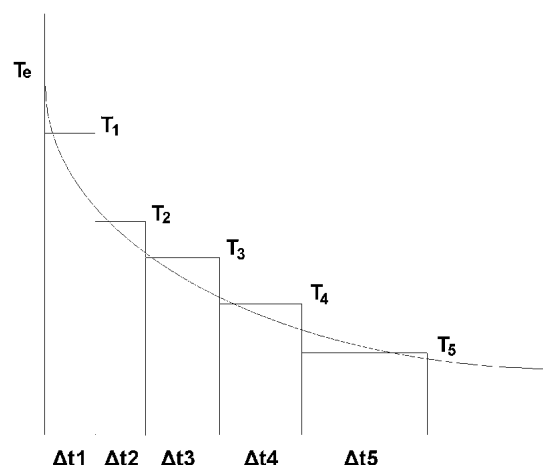


FIG. 2. Diagram showing the approximation of continuous cooling as the sum of short isothermal holding.

calculation of the driving force of ferrite nucleation for the Fe–C alloy, the driving force of ferrite nucleation  $\Delta G_{N(S)}^{\gamma \rightarrow \alpha + \gamma^1}$  to the multicomponent alloy could be written as

$$\Delta G_{N(S)}^{\gamma \rightarrow \alpha + \gamma^1} = \Delta G_S^{\gamma \rightarrow \alpha} - RT \ln a_S^\gamma \quad (4)$$

where  $\Delta G_S^{\gamma \rightarrow \alpha}$  is the free energy change of the super-element  $S$  from the  $\gamma \rightarrow \alpha$  phase transformation, and it is given by

$$\Delta G_S^{\gamma \rightarrow \alpha} = 141 \sum x_i (\Delta T_M^i - \Delta T_{NM}^i) + \Delta G_{Fe(S)}^{\gamma \rightarrow \alpha} \quad (5)$$

Here  $x_i$  is a mole fraction of a alloy element  $X_i$ ,  $\Delta T_M^i$  and  $\Delta T_{NM}^i$  are Zener parameters, which are listed in Table I.<sup>13</sup>  $\Delta G_{Fe(S)}^{\gamma \rightarrow \alpha}$  is the free energy change of Fe in the  $\gamma \rightarrow \alpha$  phase transformation, and it is given by

$$\Delta G_{Fe(S)}^{\gamma \rightarrow \alpha} = 20853.06 - 466.35T - 0.046304T^2 + 71.147T \ln T \quad (6)$$

The activity coefficient of the super-element  $S$  in austenite  $a_S^\gamma$  can be expressed as

$$\ln a_S^\gamma = \{ \ln[(1 - Z_\gamma x_C^\gamma)/(1 - x_C^\gamma)] / (Z_\gamma - 1) \} \quad (7)$$

Here  $x_C^\gamma$  is a initial mole fraction of carbon in austenite, and  $Z_\gamma$  is given by

$$Z_\gamma = 14 - 12 \exp(W_\gamma / RT) \quad (8)$$

Here  $R$  is a gas constant, and  $W_\gamma$  ( $= 1250 \text{ J/mol}$ ) is the exchange energy among carbon atoms in austenite.

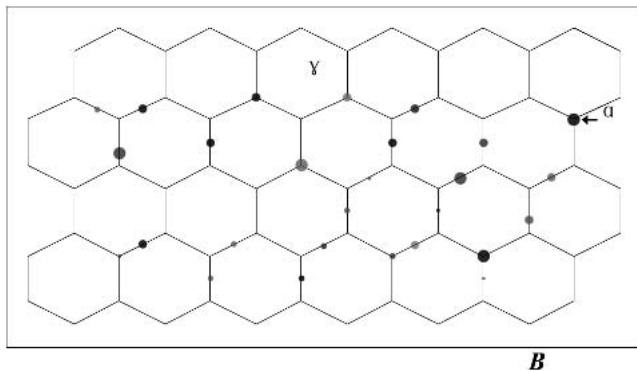


FIG. 3. Schematic diagram of the phase transformation in which ferrite nucleated on the grain boundaries of austenite.

TABLE I. Values of  $\Delta T_M^i$  and  $\Delta T_{NM}^i$  for different alloy elements.

Element	$\Delta T_M^i$ (per at.% $x_i$ )	$\Delta T_{NM}^i$ (per at.% $x_i$ )
Si	0	-3
Mn	-39.5	-37.5
Ni	-18	-6
Cu	-11.5	4.5
Cr	-18	-19

### C. Diffusion of the solute and temperature fields

The diffusion of the solute and temperature fields has a large influence on the  $\gamma \rightarrow \alpha$  phase transformation, or the phase transformation is controlled by the diffusion. Then diffusion kinetics is described as follows

$$\frac{\partial u}{\partial t} = D_u \nabla^2 u \quad (9)$$

$$\frac{\partial c_v}{\partial t} = D_v \nabla^2 c_v \quad (10)$$

$$D_\gamma \left. \frac{\partial c_\gamma}{\partial n} \right|_{\alpha/\gamma} - D_\alpha \left. \frac{\partial c_\alpha}{\partial n} \right|_{\alpha/\gamma} = v_n (c_\alpha^{\alpha/\gamma} - c_\gamma^{\alpha/\gamma}) \quad (11)$$

Here,  $t$  is time,  $c_v$  is a carbon concentration in phase  $v$  ( $\alpha$  or  $\gamma$ ), and  $D_v$  is the associated diffusion coefficient (here  $D_\gamma$  and  $D_\alpha$  are assumed to be two constants),  $c_\alpha^{\alpha/\gamma}$  and  $c_\gamma^{\alpha/\gamma}$  are two concentrations of the  $\alpha$  and  $\gamma$  domains at the  $\alpha/\gamma$  interface,  $v_n$  is the normal velocity of the  $\alpha/\gamma$  interface movement resulting from a concentration difference between  $\alpha$  and  $\gamma$  sides at the  $\alpha/\gamma$  interface, and  $n$  means the normal to this interface pointing to the  $\gamma$  side.  $D_u$  is a diffusion constant of the temperature field in  $\alpha$  and  $\gamma$  phases;  $u$  characterizes a dimensionless temperature field of the specimen,<sup>14</sup> which can be expressed as a dimensionless variable by the relation

$$u = (T - T_\infty) / (L_{at} / C_p) \quad (12)$$

where  $L_{at}$  is the latent heat of the phase transformation,  $C_p$  is the heat capacity of the multicomponent alloy, and  $T_\infty$  is the liquid temperature on the boundary  $B$  far from the studied regions as shown in Fig. 3.

### III. CELLULAR AUTOMATON MODELING

The cells of the cellular automaton are characterized by certain attributes that determine the states of one cell, and the CA evolution is defined by rules for changing the attributes. Four key features must be specified in the model: the neighborhood of a cell, boundary conditions, nucleation rules, and transition rules. The neighborhood determines which cells will be “seen” by any cell in the CA lattice. In this work, the CA is a two-dimensional hexagonal lattice with periodic boundary condition at each boundary face, and the neighborhood is defined as the nearest neighbors as seen in Fig. 4. The present simulation is two-dimensional, and the simulated results could be interpreted as what happens in a cross section of the simulated austenite or ferrite grains. Each cell in the CA lattice takes a state:  $\alpha$ ,  $\gamma$ , or “ $\alpha/\gamma$  interface” as shown in Fig. 5, and an integer in a class of integer numbers from 1 to 100 is used to represent one crystallized orientation of each cell. Then the description of the modeling procedure will be given as follows.

In the beginning of the simulation, all cells in the CA lattice are set as the  $\gamma$  phase with the same initial concentration, i.e., the composition of the alloy, and the same initial temperature  $T_{ini}$ , which is higher than  $A_{e3}$ , corresponding to the alloy composition. As the temperature is decreased at a given cooling rate  $Q$ , the temperature change of every cell is written as  $T \rightarrow T - Q \cdot \Delta t$ , where  $\Delta t$  is a time step.

*Step 1:* To a cell  $(i, j)$  on the grain boundaries of austenite with a carbon concentration  $c_{(i,j)}^\gamma$ , its  $A_{e3,(i,j)}$  corresponding to its  $c_{(i,j)}^\gamma$  is capable of being obtained from the Fe–C phase diagram. If the cell’s temperature  $T_{(i,j)}$  is decreased below  $A_{e3,(i,j)}$ ,  $T_{(i,j)} \leq A_{e3,(i,j)}$ , a

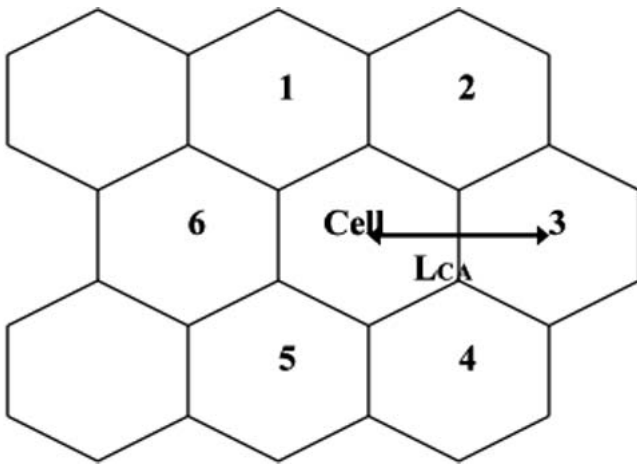


FIG. 4. One “cell” with its six neighbors 1–6.  $L_{CA}$  is the distance between two adjacent cells.

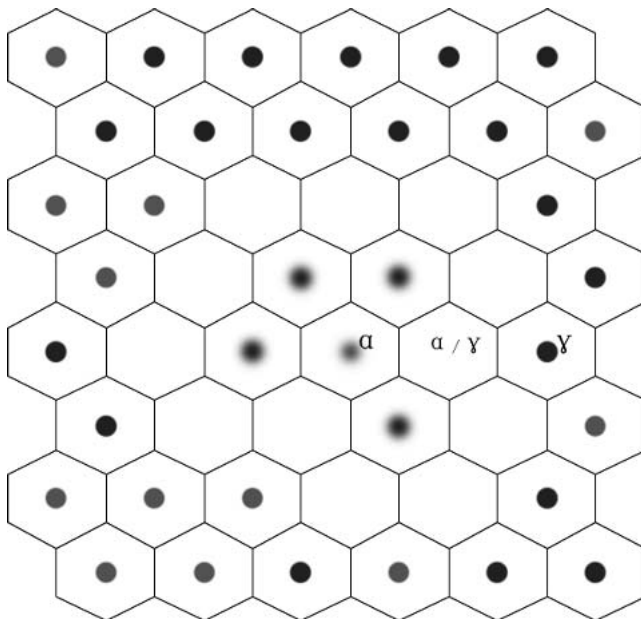


FIG. 5. Schematic illustration of  $\alpha/\gamma$  interface cells, which separate the  $\alpha$  and  $\gamma$  domains corresponding to three states ( $\alpha/\gamma$  interface,  $\alpha$  and  $\gamma$ ) of cells in the CA lattice.

nucleation probability  $p_{nuc}$  of that cell becoming ferrite is calculated as detailed in Sec. III.A. To that cell, a random number  $r_s$  ( $0 \leq r < 1$ ) is generated in advance. If  $r_s \leq p_{nuc}$  is satisfied for it, the cell will nucleate. In the meantime, it will release an amount of latent heat from the phase transformation and precipitate an amount of solutes  $\Delta c_{(i,j)}^{precipitate}$  into its neighboring austenite cells,  $\Delta c_{(i,j)}^{precipitate} = c_{(i,j)}^\gamma - c_{(i,j)}^{\alpha*}$ , where  $c_{(i,j)}^{\alpha*}$  is the concentration on ferrite phase line of the phase diagram at the temperature  $T_{(i,j)}$ . Each cell on the grain boundaries of austenite will also be scanned following the same steps as above.

*Step 2:* The cells remaining at the  $\alpha/\gamma$  interface are identified. Each  $\alpha/\gamma$  interface cell will be scanned again, based on its carbon concentration, temperature, and the states of its neighboring cells, to determine whether or not the phase transformation (nucleation or growth of its neighbor ferrite cells) can take place. In this model, the phase transformation from ferrite to austenite is not considered.

*Step 3:* Each cell transformed to ferrite from austenite, such as one cell  $(i, j)$ , will precipitate an amount of solutes into its neighboring austenite cells, and the cell  $(i, j)$  has a concentration determined by the ferrite line of the phase diagram corresponding to its temperature. Meanwhile, the cell will also release an amount of latent heat of phase transformation, and its temperature field is increased according to  $u_{(i,j)} \rightarrow u_{(i,j)} + \text{latent}$ , which “latent” is dimensionless latent heat.

*Step 4:* The diffusion of the solute and temperature fields takes place. The concentration  $c_{(i,j)}^{\gamma(\alpha \text{ or } \gamma/\alpha)}$  and the temperature field  $u_{(i,j)}$  of each cell in the CA lattice, such as one cell  $(i, j)$ , are calculated as detailed in Sec. III.B. The temperature  $T_{(i,j)}$  of the cell is given by  $T_\infty + u_{(i,j)} C_p / L_{at} \rightarrow T_{(i,j)}$ .

*Step 5:* The temperature of every cell in the CA lattice, such as one cell  $(i, j)$ , is decreased continuously,  $T_{(i,j)} - \Delta t \cdot Q \rightarrow T_{(i,j)}$ . If the temperature of one cell remaining austenite is a little lower than the temperature of cementite formation, cementite will form.

### A. Nucleation

In the present work, it is assumed a number of potential nucleating sites exists on the austenite grain boundaries, each of which can become instantaneously active when some rules are satisfied. According to Eq. (2), as there is an undercooling temperature  $\delta T = A_{e3} - T$  to one cell on the grain boundaries of austenite, a new nucleus density  $\delta n$  is given by

$$\delta n = \int_0^{\delta T} I/Q \cdot (1 - f) d\delta T \quad (13)$$

Here  $f$  takes the following value

$$f = \begin{cases} 1 & \alpha \\ (c^{\gamma*} - c)/(c^{\gamma*} - c^{\alpha*}) & \alpha/\gamma \\ 0 & \gamma \end{cases} \quad (14)$$

where  $c^{\gamma^*}$  and  $c^{\alpha^*}$  are the concentrations on the austenite and ferrite phase lines of the phase diagram, respectively, corresponding to the temperature of the studied cell as shown in Fig. 1. The nucleation probability of each cell on the grain boundaries of austenite,  $p_{\text{nuc}}$  corresponding to a possible nucleation event, is given by

$$p_{\text{nuc}} = \delta n \cdot S_{\gamma} \quad (15)$$

Here  $S_{\gamma}$  is a surface area of one cell on the grain boundaries of austenite of the specimen. To a cell on the grain boundaries of austenite, a random number  $r_s$  ( $0 \leq r_s < 1$ ) is generated. If  $r_s \leq p_{\text{nuc}}$  is satisfied for that cell, it will become ferrite or it will nucleate.

### B. Growth

Growth of ferrite is controlled by the diffusion of the solute and temperature fields, and it continues until  $A_{e3}$  of the  $\alpha/\gamma$  interface cell, such as a cell  $(i, j)$  becomes lower than its temperature  $T_{(i,j)}$  or when cementite phase forms in front of the growing ferrite grains and prevents their further growth.

#### Diffusion of the solute and temperature fields

*Step 1:* The diffusion of the solute and temperature fields among those cells of the CA lattice is described by an explicit finite approach. The change of the temperature field of the cell  $(i, j)$  during one time step  $\Delta t$  due to the diffusion could be calculated in the following way:

$$u_{(i,j)} + \frac{2\Delta t}{3L_{CA}^2} \sum_{\text{nei}=1}^6 D_u [u_{\text{nei}(i,j)} - u_{(i,j)}] \rightarrow u_{(i,j)} \quad (16)$$

where  $L_{CA}$  is the distance between two adjacent cells as shown in Fig. 4.

Calculating the diffusion of the solute field is rather more complex than that of the temperature field. Equation (17) could be used to describe the concentration variation of the  $\alpha$  cell,  $\gamma$  cell, or  $\alpha/\gamma$  interface cell  $(i, j)$  due to the diffusion from its six neighboring cells

$$c_{(i,j)} + \frac{2\Delta t}{3L_{CA}^2} \sum_{\text{nei}=1}^6 [\chi_{\text{nei}(i,j)} c_{\text{nei}(i,j)} - \chi_{(i,j)} c_{(i,j)}] \rightarrow c_{(i,j)} \quad (17)$$

*Case I:* If the cell  $(i, j)$  with its one neighboring cell nei is in the same phase  $v$  ( $\alpha$  or  $\gamma$ ),

$$\chi_{\text{nei}(i,j)} = \chi_{(i,j)} = D_v \quad (18)$$

*Case II:* If the cell  $(i, j)$  belongs to the phase  $v$ , whereas its one neighbor cell nei belongs to the interface,

$$\chi_{\text{nei}(i,j)} = D_v \cdot c_{\text{nei}(i,j)}^v / c_{\text{nei}(i,j)} \text{ and } \chi_{(i,j)} = D_v \quad (19)$$

*Case III:* If both the cell  $(i, j)$  and its one neighboring cell nei belong to the interface,

$$\chi_{\text{nei}(i,j)} = [\bar{f}^{\alpha} D_{\alpha} c_{\text{nei}(i,j)}^{\alpha^*} + (1 - \bar{f}^{\alpha}) D_{\gamma} c_{\text{nei}(i,j)}^{\gamma^*}] / c_{\text{nei}(i,j)}$$

and

$$\chi_{(i,j)} = [\bar{f}^{\alpha} D_{\alpha} c_{(i,j)}^{\alpha^*} + (1 - \bar{f}^{\alpha}) D_{\gamma} c_{(i,j)}^{\gamma^*}] / c_{(i,j)} \quad (20)$$

with

$$\bar{f}^{\alpha} = \frac{f_{(i,j)}^{\alpha} + f_{\text{nei}(i,j)}^{\alpha}}{2} \quad ,$$

here  $f_{(i,j)}^{\alpha}$  or  $f_{\text{nei}(i,j)}^{\alpha}$  is calculated by

$$f_{(i,j)}^{\alpha} = \frac{c_{(i,j)}^{\gamma^*} - c_{(i,j)}}{c_{(i,j)}^{\gamma^*} - c_{(i,j)}^{\alpha^*}} \text{ or } f_{\text{nei}(i,j)}^{\alpha} = \frac{c_{\text{nei}(i,j)}^{\gamma^*} - c_{\text{nei}(i,j)}}{c_{\text{nei}(i,j)}^{\gamma^*} - c_{\text{nei}(i,j)}^{\alpha^*}} \quad (21)$$

where  $c_{(i,j)}^{\gamma^*}$  or  $c_{(i,j)}^{\alpha^*}$  [ $c_{\text{nei}(i,j)}^{\gamma^*}$  or  $c_{\text{nei}(i,j)}^{\alpha^*}$ ] is the concentration of the cell  $(i, j)$  (its one neighbor cell) on the austenite phase line or the ferrite phase line of the phase diagram at the temperature  $T_{(i,j)}$  [ $T_{\text{nei}(i,j)}$ ].

*Step 2:* At time  $t$ , a growth length  $l_{(i,j) \rightarrow \text{nei}}^{(i,j)}$  of the ferrite cell  $(i, j)$  toward its one neighboring  $\alpha/\gamma$  interface cell nei is calculated by

$$l_{(i,j) \rightarrow \text{nei}}^{(i,j)}(t) = \int_{t_0}^t v_{(i,j) \rightarrow \text{nei}}^{(i,j)} dt \quad (22)$$

Here  $t_0$  is the time of the cell  $(i, j)$  becoming ferrite, and  $v_{(i,j) \rightarrow \text{nei}}^{(i,j)}$  is the growing velocity of the cell  $(i, j)$  toward the neighbor cell nei and it can be calculated by Eq. (11).

*Step 3:* The time step  $\Delta t$  is an important measure in modeling because the state of each cell is changed rhythmically with its increase, and it could be defined as

$$\Delta t = \frac{1}{5} \min \left( \frac{L_{CA}}{v_{\text{max}}}, \frac{L_{CA}^2}{D_u}, \frac{L_{CA}^2}{D_{\alpha}}, \frac{L_{CA}^2}{D_{\gamma}} \right) \quad (23)$$

where  $v_{\text{max}}$  is the maximum among the growth velocities of all ferrite cells and “min” means the minimum value of four ones in the round bracket.

*Step 4:* For a rapid cooling procedure, the relationship between growth of ferrite and the solute diffusion must be taken into account. The growth time step  $\Delta t_{\text{grow}}^{(i,j) \rightarrow \text{nei}}$  of one ferrite cell  $(i, j)$  toward its one neighbor  $\alpha/\gamma$  interface cell nei calculated by  $\Delta t_{\text{grow}}^{(i,j) \rightarrow \text{nei}} = L_{CA} / v_{(i,j) \rightarrow \text{nei}}^{(i,j)}$ . If it is smaller than the time step of solute diffusion in austenite  $\Delta t_{\text{diff}}$  ( $\Delta t_{\text{diff}} = L_{CA}^2 / D_{\gamma}$ ), there the solute diffusion exists in cell nei during growth of the ferrite cell. However, if  $\Delta t_{\text{diff}} \geq \Delta t_{\text{grow}}^{(i,j) \rightarrow \text{nei}}$ , growth could have already finished for the ferrite cell  $(i, j)$  toward the cell nei before the solute diffusion in the cell nei would be able to take place.

*Step 5:* For an  $\alpha/\gamma$  interface cell nei, if its temperature  $T_{(i,j)}$  is lower than its  $A_{e3,(i,j)}$  and its generated “transformed” probability  $r_{tra}$  ( $0 \leq r_{tra} < 1$ ) is smaller than a “capture” probability  $p_{cap}^{(i,j) \rightarrow nei}$  of its neighbor ferrite cell  $(i, j)$  toward the cell nei, the cell nei will become ferrite. The capture probability  $p_{cap}^{(i,j) \rightarrow nei}$  is given by

$$p_{cap}^{(i,j) \rightarrow nei} = \frac{l_{(i,j)}^{(i,j) \rightarrow nei}}{L_{CA}} \quad (24)$$

### C. Cementite formation

As the temperature decreases, more and more ferrite forms, and carbon solutes build up in front of the growing ferrite grains. Thus, many cells become undercooled with respect to cementite formation, and the formed cementite will stop growth of the ferrite grains.

## IV. RESULTS AND DISCUSSIONS

Figures 6(a)–6(b) show the microstructure evolution and final morphology—from nucleation of the ferrite cells on the austenite grain boundaries and growth of the nucleated ferrite cells toward their neighbor austenite cells—of a Fe– $\Sigma X_i$  alloy [chemical composition (wt%): C 0.15, Si 0.09, Mn 0.4, Cr 0.02, Ni 0.02, Cu 0.01] under continuous cooling ( $Q = 1.0$  K/s) from temperature 1320 K to the final temperature, room temperature. Different colors (replaced by the different grey scales in black and white pictures) in the figures represent the different austenite or ferrite grains. The modeled specimen size is  $0.6 \times 0.6$  mm (corresponding to  $200 \times 200$  cells).

In the beginning, a few ferrite grains nucleate on the grain boundaries of austenite [as shown in Fig. 6(a); some nucleation sites of ferrite are marked by white squares]. Then, as the temperature is decreased, the

nucleated ferrite grains begin to grow, and more and more ferrite grains nucleate [Fig. 6(b)]. Finally, Fig. 6(c) displays the morphology with many large and small ferrite grains.

As described in Sec. II.A., the model assumes that ferrite grains nucleate on the boundaries of austenite grains, thus each cell on the boundaries of austenite grains is a potential nucleation site. Under cooling, the nucleation probability of ferrite becomes large for each potential nucleation site, and it means that many cells may nucleate. Nevertheless, the nucleated ferrite cells will precipitate an amount of solutes into their neighboring austenite grains and release certain latent heat. Therefore, the concentrations of the austenite cells neighboring upon the ferrite grains become enriched. In addition, those of the other austenite cells (inner austenite grains and on the boundaries of austenite grains), which do not neighbor upon the ferrite grains, may also be increased for the solute diffusion. In the meantime, the temperature of the austenite cells will become high, resulting from the temperature field diffusion. For those austenite cells, equilibrium temperatures beginning at the phase transformation  $A_{es}$  could be decreased because their concentrations are increased from the solutal diffusion or receiving precipitated solutes, but their actual temperatures are increased from the thermal diffusion. At a given time, the equilibrium temperatures beginning at the phase transformation of some austenite cells may be lower than their actual temperatures. Therefore, because undercooling temperatures ( $\Delta T = A_{es} - T$ ) of the cells remaining austenite are decreased, the nucleation probabilities of the potential nucleation cells on the grain boundaries of austenite are also decreased. Simply stated, diffusion affects nucleation of ferrite. Meanwhile, although the austenite cells may not nucleate, they will be able to become ferrite, resulting from growth of their neighboring ferrite cells. Growth of ferrite grains can proceed if

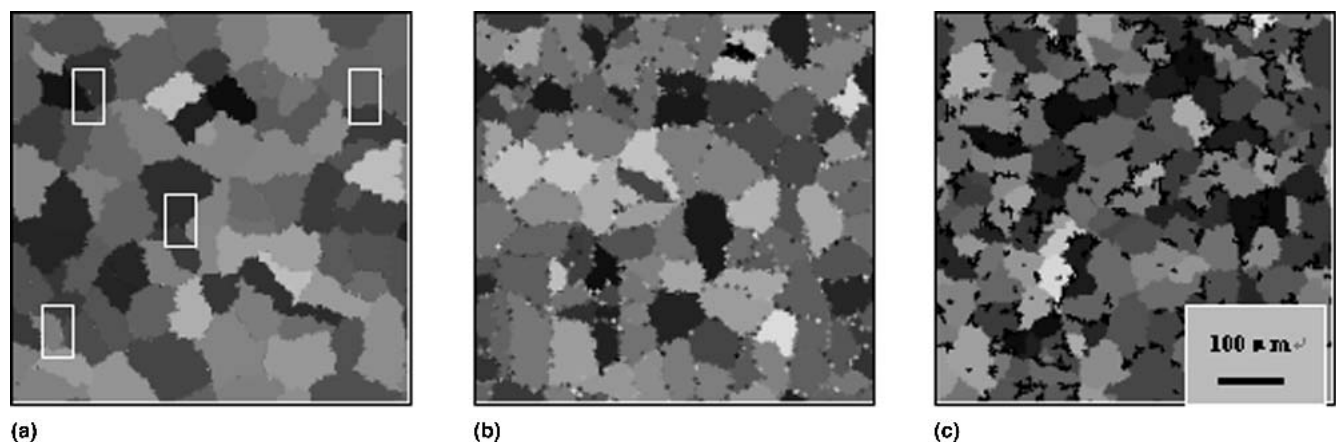


FIG. 6. Ferrite grains nucleating on the surface of the austenite grains and their growth under the cooling rate  $Q = 1$  K/s. The final temperature of the sample is room temperature. (a), (b), and (c) correspond to the three stages of nucleation beginning on the grain boundaries of austenite, phase transformation processing and the final ferrite grain structure. In (a), some nucleation sites of ferrite are marked by white squares ( $\square$ ).

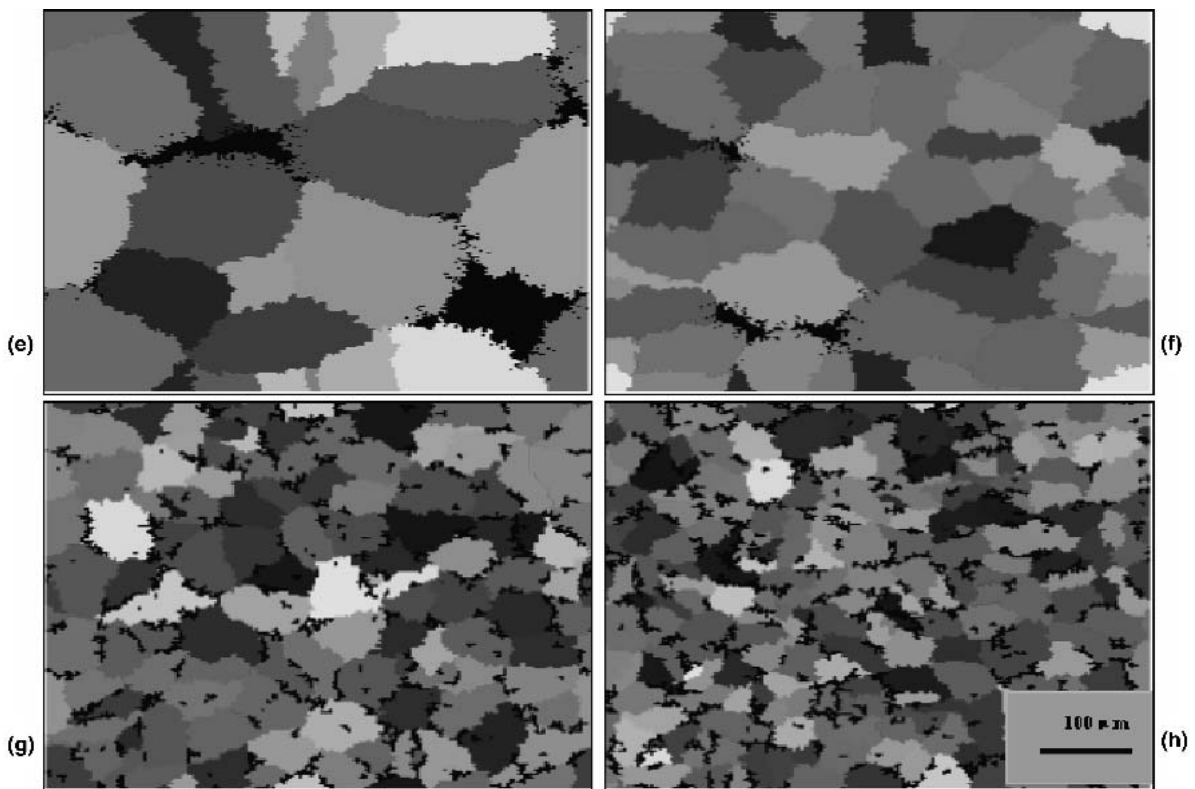
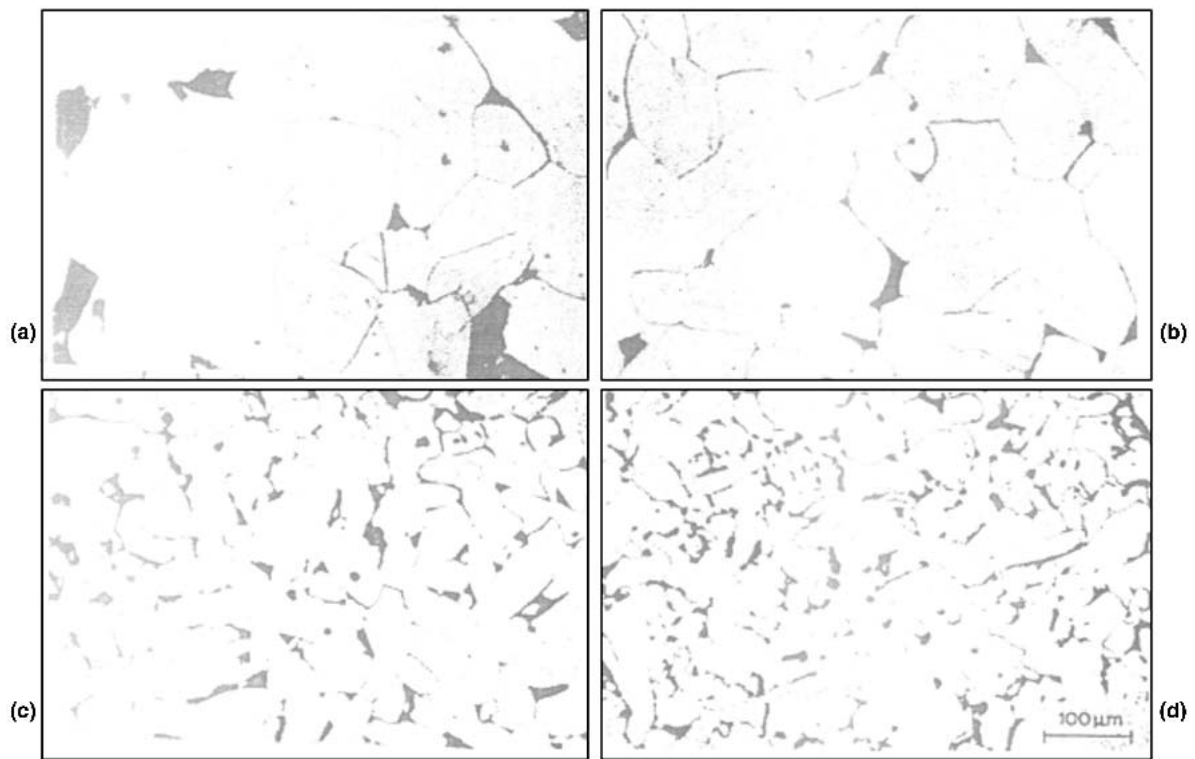


FIG. 7. With the same initial austenite grain structure, the different cooling rates have effects on the final grain structure of ferrite. (a–d) Optical micrographs showing ferrite grains formed at various cooling rates: (a)  $Q = 0.05$  K/s,  $d_{\alpha} = 106$  μm; (b)  $Q = 0.17$  K/s,  $d_{\alpha} = 79$  μm; (c)  $Q = 1.5$  K/s,  $d_{\alpha} = 48$  μm; and (d)  $Q = 5.0$  K/s,  $d_{\alpha} = 33$  μm). (e–h) Simulated structures corresponding to the cooling rates  $Q = 0.05$  K/s,  $Q = 0.17$  K/s,  $Q = 1.5$  K/s, and  $Q = 5.0$  K/s; (e)  $d_{\alpha} = 108$  μm, (f)  $d_{\alpha} = 75$  μm, (g)  $d_{\alpha} = 43$  μm, and (h)  $d_{\alpha} = 38$  μm.

undercooling temperatures exist in their neighboring austenite cells and cementite does not form in front of the growing ferrite grains. Certainly, growth of the ferrite grains is also affected by the diffusion of the solute and temperature fields for which uniform distribution of the solute and temperature fields is a great help to sufficient growth of the ferrite grains. If the given cooling rate is small enough, the uniformity structure of ferrite grains could be obtained. However, because the cooling rate could not be small enough in the model, distribution of the solute or temperature fields is not uniform in the modeled specimen. Then the number of the nucleated ferrite grains may be large in some zones of the specimen, or the ferrite grains might grow more quickly in the other zones. Thus, the final structure as shown in Fig. 6(c) is obtained, where the size of some grains is larger than that of others, and the resultant ferrite grain size is not uniform. In general, the diffusion of the solute and temperature fields plays an important role in nucleation and growth, or nucleation and growth is diffusion-controlled. Besides these grains there are some small deep black regions inside ferrite grains or on the grain boundaries of ferrite, which are cementite. The formation of cementite could be understood by the following fact: The small regions are enriched in solutes while the ferrite phase forms around them. Before the enriched solutes can diffuse, the temperatures of the regions remaining austenite decrease down the temperature of cementite formation; then cementite phase forms in the regions.

Figure 7 displays the effect of the cooling rate on the resultant structure of ferrite grains under the same initial austenite grain size (126  $\mu\text{m}$ ) from the temperature 1323 K, and the final temperature is room temperature. Figures 7(a)–7(d)<sup>2</sup> are the optical micrographs that show ferrite grains formed by continuous cooling transformation at various rates, and Figs. 7(e)–7(h) are the simulated microstructure of ferrite grains at those rates. From the figures, we can clearly see that a large cooling rate makes the ferrite grain size finer than a small cooling rate does. The phenomenon can be explained by the following. To make the ferrite grain size uniform and fine, increasing nucleation number and controlling growth of ferrite are two efficient ways. If the cooling rate is small, the diffusion of the solute field could go on a quite long time. The average concentrations of the cells remaining austenite become high because they receive the precipitated solutes from the ferrite grains. Then their equilibrium temperatures beginning at the phase transformation become lower. In some cases, because their temperatures are higher than their equilibrium temperatures beginning at the phase transformation, they cannot nucleate. Nevertheless, under rapid cooling, the temperature is decreased down to quite a low level (which is much lower than the equilibrium temperature beginning at

phase transformation corresponding to the alloy composition). At this time, many potential nucleation sites on the grain boundaries of austenite could become ferrite as there exist undercooling temperatures for them, and the large undercooling temperatures also make nucleation probabilities of those potential sites high. Thus, the final nucleation sum of ferrite increases because the sum of the potential nucleation cells and the nucleation probabilities of them are both improved. In addition to the nucleation number increased, the diffusion of the solute and temperature fields also has a great influence on growth of the ferrite grains. Because the diffusion of the temperature field is much quicker than that of the solute field and the temperature distribution becomes quickly uniform to the small modeled specimen, the diffusion of the solute field has larger influence on nucleation and growth of ferrite. At a small enough cooling rate, the concentration distribution could be uniform due to enough diffusion of the solute field. At a large cooling rate, before diffusion of solute field could take place, the growth of the ferrite grains toward their neighboring austenite cells could have finished. Because the temperature decreases quickly, however, the cementite phase would form in front of the growing ferrite grains and it would stop their further growth if the temperature were lower than the temperature of cementite formation to the enriched solute cells neighboring them. Thus, the grain size of ferrite is not able to become very large, and the uniformity and fine grain size of ferrite is formed. According to this, the morphologies shown in Figs. 7(d)–7(h) corresponding to the cooling rates  $Q = 0.05$  K/s,  $Q = 0.17$  K/s,  $Q = 1.25$  K/s, and  $Q = 5.0$  K/s, respectively, are calculated. Figure 8 illustrates the variation of the average grain size of ferrite to the different cooling rates. Here, the average grain size of ferrite  $d_\alpha$  is calculated by  $d_\alpha = \frac{\sum_{i=1}^{\text{num}} d_\alpha^i}{\text{num}}$  ( $\text{num}$  is the number of the ferrite grains, and  $d_\alpha^i$  is the grain size of the  $i$ th ferrite

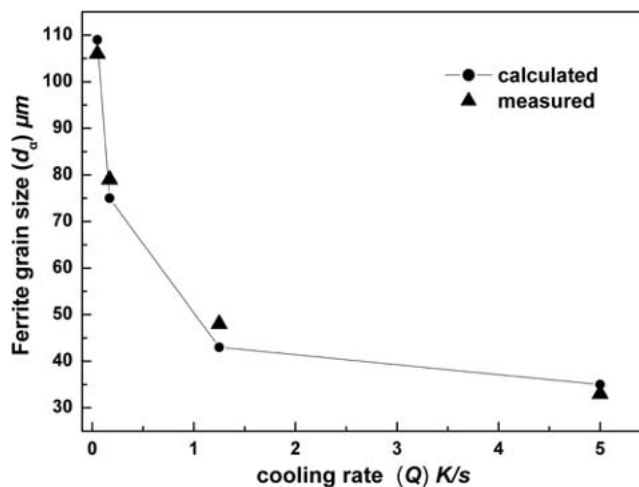


FIG. 8. Effect of cooling rate on ferrite grain size.

grain). The figure indicates that the quicker the cooling rate is, the finer the final grain size of ferrite is after the phase transformation.

## V. CONCLUSION

A two-dimensional cellular automaton model has been developed to model the combined complex behavior of heat–mass transfer, nucleation of ferrite, and growth of nucleated grains during the  $\gamma$ – $\alpha$  phase transformation of low-carbon steels. This modeling gives us physical insight into how dynamically they interact and constrain each other and what their combined effects on the microstructural evolution are. The simulated results are compared with the optical micrographs showing ferrite grains formed at various cooling rates, and they are in good agreement with those micrographs. Moreover, CA modeling can demonstrate the microstructural evolution of multigrains involving nucleation and growth in nearly reality, and it can, also give the microstructure at any time. Nevertheless, it is investigated only through experiments, The phase transformation of the low carbon steel Fe– $\Sigma X_i$ –C is proven to be a mass–heat diffusion-controlled process, and the diffusion processes have an important influence on the nucleation and growth, and in turn, the microstructure formation of ferrite grains. With the same initial grain size, the final morphology of ferrite depends mainly on the cooling rate during the phase transformation. A larger cooling rate is a great help to obtain finer ferrite grains in the CA model, which is in agreement with experiment. Thus, it is concluded that the present model can evaluate the  $\gamma$ – $\alpha$  phase transformation

of low-carbon steels. In addition, the time step  $\Delta t$  [Eq. (23)] selected is proven to be an important measure for correctly simulating the phase transformation in the CA model.

## ACKNOWLEDGMENT

We acknowledge financial support of this work by the Key Project of the National Fundamental Research of China under the Grant No. G1998061509.

## REFERENCES

1. M. Umemoto, H. Ohtsuka, and I. Tamura, *Acta Metall.* **34**, 1377 (1986).
2. M. Umemoto, Z.H. Guo, and I. Tamura, *Mater. Sci. Technol.* **3**, 249 (1987).
3. A. Jacot and M. Rappaz, *Acta Mater.* **45**, 575 (1997).
4. M. Kumar, R. Sasikumar, and P.K. Nair, *Acta Mater.* **46**, 6291 (1998).
5. W.F. Lange, III, M. Enomoto, and H.I. Aaronson, *Metall. Trans.* **19A**, 429 (1988).
6. M. Militzer, R. Pandi, and E.B. Hawbolt, *Metall. Mater. Trans. A*, **27A**, 1547 (1996).
7. M. Rappaz and Ch-A. Gandin, *Acta Metall.* **41**, 345 (1993).
8. Ch. Charbon, A. Jacot, and M. Rappaz, *Acta Metall.* **42**, 3953 (1994).
9. S.A. Spittle and S.G.R. Brown, *J. Mater. Sci.* **30**, 3989 (1995).
10. M.F. Zhu and C.P. Hong, *ISIJ* **41**, 436 (2001).
11. S. Wolfram, *Phys. D* **10D**, 7 (1984).
12. H.K.D.H. Bhadeshia, *Met. Sci.* **15**, 178 (1981).
13. H.I. Aaronson, H.A. Domian, and G.M. Pound, *TMS-AIME* **236**, 753 (1966).
14. Y. Saito, G. Goldbeck-Wood, and H. Muller-Krumbhaar, *Phys. Rev. A* **38**, 214 (1998).